Audio Engineering Society

Convention Paper 10409

Presented at the 149th Convention
Online, 2020 October 27-30

Individual Listening Zone with Frequency-Dependent Trim of Measured Impulse Responses

Michele Ebri[1], Nicolò Strozzi[2], Filippo Maria Fazi[3], Angelo Farina[1], and Luca Cattani[2]

[1]*University of Parma*
[2]*ASK Industries Spa*
[3]*University of Southampton*

Correspondence should be addressed to Michele Ebri (michele.ebri@unipr.it)

ABSTRACT

Acoustic Contrast Control (ACC) has been widely used to achieve individual audio delivery in shared environments. The effectiveness of this method is reduced when the control is performed in reverberant environments. Even if control filters are computed using measured transfer functions, the robustness of the system is affected by the presence of reverberation in the plant matrix. In this paper a new optimization method is presented to improve the ACC algorithm by applying a frequency-dependent windowing of the measured impulse response used for the filter computation, thus removing late reflections. The effects of this impulse response optimization are presented by means of sound zoning results obtained from experimental measurements performed in a car cabin.

1 Introduction

Various mathematical models have been developed in the last decades to face the problem of sound field control and sound zoning. The Pressure Matching (PM) is one of the most common least-square approaches to perform channel inversion-based sound field synthesis [1], whereas the Acoustics Contrast Control (ACC) [2] has been conceived to maximize the sound pressure difference between two target zones, namely the bright and the dark zone. These methods are subject to several constraints and limitations in real environments [3, 4]. The purpose of this paper is to define an optimal method to improve the filters quality in terms of filter energy dispersion, and the system robustness in order to achieve the highest possible acoustics contrast between two target zones. The above mentioned limitations represent a critical issue in reverberant environments, therefore this work will address the filter optimization problem in a car cockpit. Previous works based on the ACC method to perform in-car sound zoning have already shown the impact of these limitation [5, 6, 7]. In fact, the reverberant measurement-based sound zone separation leads to an ill-conditioned problem, whose solution leads to unstable and long control filters. These sound zoning approaches reliability has been extensively discussed in the literature [8, 9, 10], but the poor robustness of the solution has been usually tackled by increasing the regularization parameter during the inversion process. In this paper an Acoustic Contrast (AC) optimization is achieved by manipulating the measured transfer function matrix. The proposed method is based on separating the direct component and early reflections of the measured impulse responses from the late reflections. This is performed by applying a frequency-dependent windowing in the time domain, hereafter also referred

to as trimming. This approach makes it possible to neglect those impulse response's components that lead to poor robustness without compromising the sound field control performances. The optimal window length, which has to be applied in order to obtain the optimal results in term of acoustic contrast and filter quality, has been investigated by analysing the trimming effect over different impulse responses.

This paper is organized as follows: in Section 2 an overview on the acoustic contrast control algorithm is presented. In Section 3, the proposed optimization, based on the impulse response trim, is provided. In Section 4 the experimental setup is presented highlighting the in-car instrumentation and the acquisition strategies. In Section 5 the results obtained with the proposed approach are compared with the ones based on the not-trimmed impulse responses. Finally, in Section 6, the conclusions on this work are provided.

2 Acoustic Contrast Control

The ACC approach, proposed by Choi and Kim in [2], aims to maximize the sound pressure level difference between two zones by using L loudspeakers and M_B and M_D microphones, or control points, in the bright and the dark zone, respectively. The goal is to maximize the acoustic contrast considering the measured sound pressure in the bright zone and in the dark zone, which are expressed for each frequency by the vectors $\mathbf{y}_B$ and $\mathbf{y}_D$, of dimensions M_B and M_D, respectively. The acoustic contrast used for this optimisation is defined, in the frequency domain, as

$$AC = \frac{M_D \mathbf{y}_B^H \mathbf{y}_B}{M_B \mathbf{y}_D^H \mathbf{y}_D} = \frac{M_D \mathbf{u}^H \mathbf{G}_B^H \mathbf{G}_B \mathbf{u}}{M_B \mathbf{u}^H \mathbf{G}_D^H \mathbf{G}_D \mathbf{u}} \tag{1}$$

where $\mathbf{u}$ are the loudspeaker filters, expressed in the frequency domain and corresponding to the loudspeaker driving signals for a unitary pulse input signal. $\mathbf{G}_B$ is the $M_B \times L$ matrix of impulse responses in the frequency domain between L loudspeakers and M_B microphones in the bright zone, whereas $\mathbf{G}_D$ is the $M_D \times L$ analogous matrix for M_D microphones in the dark zone. The complex microphone signals are therefore given by

$$\mathbf{y}_B = \mathbf{G}_B \mathbf{u} \tag{2}$$

$$\mathbf{y}_D = \mathbf{G}_D \mathbf{u} \tag{3}$$

The maximization problem to be solved is

$$\arg\max_{\mathbf{u}} AC \quad s.t. \ \mathbf{u}^H \mathbf{G}_B^H \mathbf{G}_B \mathbf{u} = B \tag{4}$$

The constraint is applied to set a proper average target sound pressure level B on the bright zone.

This problem corresponds to the indirect formulation discussed by Elliot *et al.* in reference [8]. This is formulated in terms of the eigenvalue problem

$$\frac{1}{\lambda_1}\mathbf{u} = -[\mathbf{G}_D^H \mathbf{G}_D + \beta \mathbf{I}]^{-1} [\mathbf{G}_B^H \mathbf{G}_B]\mathbf{u} \tag{5}$$

where β is the regularization parameter introduced to improve the stability of the solution and λ_1 is the Lagrange multiplier related to the level constraint introduced in (4). The filters vector $\mathbf{u}$ is proportional to the eigenvector $\hat{\mathbf{u}}$ corresponding to the largest eigenvalue λ_1^{-1}. Since $||\hat{\mathbf{u}}|| = 1$, it is necessary to multiply it by a proper coefficient, for each frequency, in order to reach the chosen average sound pressure level B in the bright zone. This rescaling operation is

$$\mathbf{u} = \hat{\mathbf{u}} \sqrt{\frac{B}{B'}} \tag{6}$$

where $B' = \hat{\mathbf{u}}^H \mathbf{G}_B^H \mathbf{G}_B \hat{\mathbf{u}}$.

2.1 Control Parameters

To evaluate the ACC filters performance fairly it is necessary to take into account several indicators. In this paper the following metrics are adopted to provide a exhaustive overview: (i) the acoustic contrast AC between the bright and the dark zone, (ii) the control filters effort E, and (iii) the control filters compactness estimated by means of I, namely the central moment of the normalized energy temporal density.

2.1.1 Acoustic Contrast

The acoustic contrast AC represents the sound pressure level difference between the bright and the dark zone. In order to avoid unfair performance analysis by evaluating the filters $\mathbf{u}$ at the same control points chosen to estimate the filters themselves, we have used two different set of transfer function. The first set $\{\mathbf{G}_B, \mathbf{G}_D\}$ consist of the transfer functions, measured by the $\{M_B, M_D\}$ microphones, used to compute the filters, whereas $\{\mathbf{G}'_B, \mathbf{G}'_D\}$ are the transfer function,

measured by the $\{M'_B, M'_D\}$ microphones, used to estimate the sound separation performance in terms of *AC* (details on the measurement setup are provided in Section 4). By using this notation, the AC' is defined, for each frequency, as:

$$AC' = 10 \cdot \log_{10} \left(\frac{M'_D \mathbf{u}^H \mathbf{G'}_B^H \mathbf{G'}_B \mathbf{u}}{M'_B \mathbf{u}^H \mathbf{G'}_D^H \mathbf{G'}_D \mathbf{u}} \right) \quad (7)$$

Note that this is different from eq. (1) because different sets of control microphones are used and the logarithmic scale has been considered in order to simplify the data analysis. In real reverberant scenarios, the transfer functions $\{\mathbf{G}'_B, \mathbf{G}'_D\}$ present high amplitude and phase variability which decreases the readability of the AC' parameter over the whole spectrum. This has led to the definition of a third-octave acoustic contrast parameter AC^{oct} which is expressed for each band as

$$AC_k^{oct} = 10 \cdot \log_{10} \left(\frac{M'_D \varepsilon_{B,k}^{oct}}{M'_B \varepsilon_{D,k}^{oct}} \right) \quad (8)$$

where $\varepsilon_{B,k}^{oct}$ and $\varepsilon_{D,k}^{oct}$ are the k-th third-octave band average of of $\mathbf{u}^H \mathbf{G'}_B^H \mathbf{G'}_B \mathbf{u}$ and $\mathbf{u}^H \mathbf{G'}_D^H \mathbf{G'}_D \mathbf{u}$, respectively.

2.1.2 Array Effort

A well known parameter broadly adopted to evaluate the loudspeaker array energy required for the sound control algorithms is the array effort AE. This parameter is defined as

$$AE = \frac{\mathbf{u}^H \mathbf{u}}{|u_R|^2} \quad (9)$$

where u_R is the source strength needed to obtain the target sound pressure in the bright zone by using an ideal monopole source positioned in the array centre. The higher is the array effort value the higher will be the loudspeaker dynamic range necessary to avoid non linear effects. Also, a large array effort is an indicator of poor system robustness against errors.

2.2 Filter Compactness

In acoustic application it is necessary to take into account the filter quality in order to avoid perceivable defects, such as noise, pre-ringing or filter energy spread over time. These unwanted effects are usually introduced when the ACC filter computation is based on transfer functions measured in real reverberant environments. In this paper the quality of control filters is evaluated by analysing their compactness in the time domain. The parameter introduced to quantify the filter quality is the central moment of the normalised energy temporal density I. We define

$$E = \sum_n h_n^2 \quad (10)$$

$$C = \sum_n n \frac{h_n^2}{E} \quad (11)$$

$$I = \sum_n (n - C)^2 \frac{h_n^2}{E} \quad (12)$$

where h_n is the amplitude of the n-th sample of a given filter in the time domain, the latter being the inverse Fourier transform of one element of vector $\mathbf{u}$. This parameter is an indicator of the filter compactness in the time domain, for almost symmetrical filters, such as the ones obtained from ACC algorithms. For instance, a Dirac delta has I equal to 0. In general, the more the filter energy is spread in the time the more I value will increase.

3 Acoustic Contrast Optimisation with Impulse Response Trimming

In reflective environments, the filters computed by sound zoning algorithms lead to long control filters that are often not very robust [3, 4]. In this case, errors caused by the high variability of the impulse responses due to modification in the environment such as microphone or loudspeaker displacement, system geometry changes may have major effect on the system performance. The presence of multiple reflections in transfer functions results in poor sound control especially at high frequencies, where the transfer function variability is highly dependent on small geometrical and physical variations of the environment.

The solution proposed in this paper will tackle this problem by improving the system robustness and acoustic contrast performances exploiting a specific trim of the measured impulse responses used for ACC algorithms. The idea is to remove from the ACC filters calculation those components of $\{\mathbf{G}_B, \mathbf{G}_D\}$ that are related to late reflections, that vary significantly depending on the position of the control points, i.e. a microphone placement. The impulse response is divided into two parts: the first part, that can be considered to include

the direct component and the early reflections reaching the microphone, and the second part including the late reflections, which can be considered as uncorrelated to the first part and, especially in a small environment as a car cockpit, are very sensitive to changes of the environment. It must also be ensured, however, that the benefit obtained by removing the late part of the impulse responses is not offset by a significant degradation of the system performance in terms of acoustic contrast. With this in mind, it is necessary to apply a frequency-dependent trim of the measured impulse responses. In this paper the time length of the first component defined above will be evaluated for each frequency as the one which provide the best sound field control performance.

The frequency-dependent trim is based on the definition of the optimal trimming length N^{oct} for each third-octave frequency band. The choice of these optimal values was carried out by comparing the AC performance of the different filters computed with impulse responses trimmed with different window lengths. The detail of this choice is discussed in the next session. Once defined N^{oct} for each third-octave band, a given impulse response in the time domain $\mathbf{g}_{m,\ell}$ is trimmed through a time window filter $\mathbf{w}^{oct}$ specific for the considered third-octave band. We underline that $\mathbf{g}_{m,\ell}$ is computed by applying the inverse Fourier transform of the corresponding element of the plant matrix $\mathbf{G}$. Therefore, a zero phase rectangular band-pass filter $\mathbf{f}^{oct}$, centered on a specific third-octave band, is applied to the trimmed impulse response. This lead to the definition of the filter $\tilde{\mathbf{g}}^{oct}_{m,\ell}$, namely the specific third-octave component of the trimmed impulse response. As shown in the flow chart in Fig. 1, by repeating this procedure on $\mathbf{g}_{m,\ell}$ for each third-octave component and computing the summation of all the resulting $\tilde{\mathbf{g}}^{oct}_{m,\ell}$, the final trimmed impulse response $\tilde{\mathbf{g}}_{m,\ell}$ is generated:

$$\tilde{\mathbf{g}}^{oct}_{m,\ell} = (\mathbf{g}_{m,\ell} \odot \mathbf{w}^{oct}) \otimes \mathbf{f}^{oct} \tag{13}$$

$$\tilde{\mathbf{g}}_{m,\ell} = \sum_{oct=1}^{T} \tilde{\mathbf{g}}^{oct}_{m,\ell} \tag{14}$$

where $\odot$ represents the element-wise (Hadamard) product between two vectors, $\otimes$ represent convolution in time domain which was actually implemented as a multiplication in the frequency domain and T represents the total number of third-octave bands considered in the computation.

Each element of the "trimmed" transfer function matrix $\tilde{\mathbf{G}}$ is finally computed by performing the Fourier

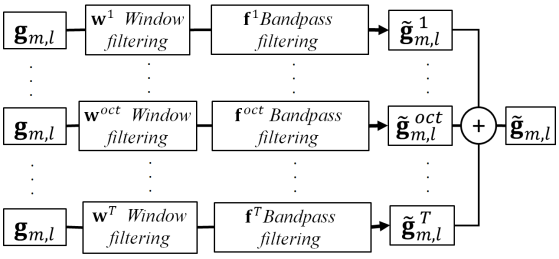

Fig. 1: Frequency dependent trimming flow chart

transform of the trimmed filters. An example of the frequency dependent trim is shown in Fig. 2, where a measured impulse response (a) is compared with its trimmed version (b), choosing $N^{oct} = \frac{10}{f_c^{oct}}$ for each third-octave band, where f_c^{oct} is the central frequency of each specific band. It can be seen from the impulse response spectrogram shown in Fig. 3 that choosing these specific N^{oct} values, the low frequencies are essentially not trimmed, while the high-frequency late-reflections components have been removed.

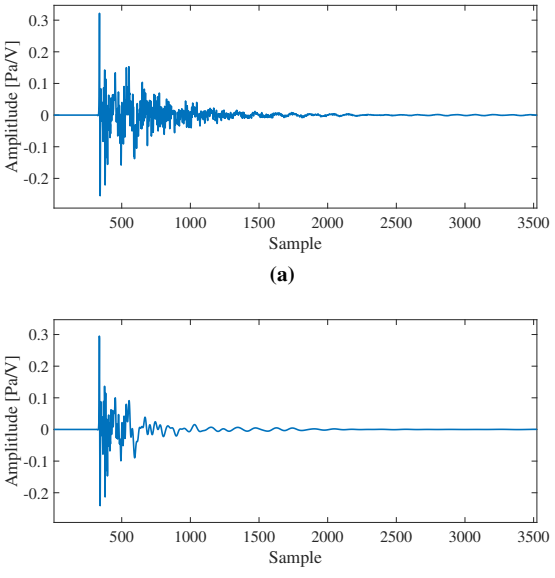

Fig. 2: Impulse response before (a) and after (b) the frequency-dependent trim with $N^{oct} = \frac{10}{f_c^{oct}}$

Once the trimmed transfer function matrices $\{\tilde{\mathbf{G}}_B, \tilde{\mathbf{G}}_D\}$ have been generated, equations (1) and (4), which describe the ACC maximization problem, are redefined

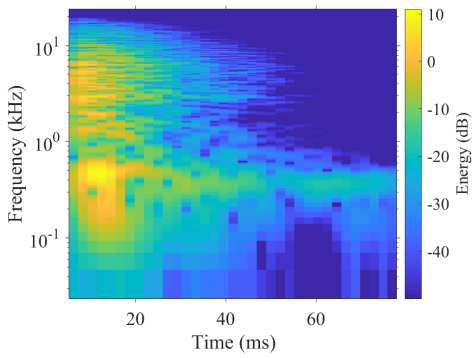

Fig. 3: Spectrogram of impulse response before (a) and after (b) the frequency-dependent trim with $N^{oct} = \frac{10}{f_c^{oct}}$

as follows:

$$\tilde{AC} = \frac{M_D \mathbf{u}^H \tilde{\mathbf{G}}_B^H \tilde{\mathbf{G}}_B \mathbf{u}}{M_B \mathbf{u}^H \tilde{\mathbf{G}}_D^H \tilde{\mathbf{G}}_D \mathbf{u}} \tag{15}$$

$$\arg\max_{\mathbf{u}} (\tilde{AC}) \quad s.t. \quad \mathbf{u}^H \mathbf{G}_B^H \mathbf{G}_B \mathbf{u} = B \tag{16}$$

Note that the sound pressure level constraint is identical to that in equation (4). The solution of this problem is an eigenvector of

$$\frac{1}{\lambda_1}\mathbf{u} = -[\tilde{\mathbf{G}}_D^H \tilde{\mathbf{G}}_D + \beta \mathbf{I}]^{-1} [\tilde{\mathbf{G}}_B^H \tilde{\mathbf{G}}_B]\mathbf{u} \tag{17}$$

and its magnitude is defined by equation (6).

4 Experimental Measurements

A real scenario to evaluate the effect of a frequency-dependent trim on reverberant impulse responses was analysed in a real scenario. The chosen environment is the interior of a car. The presence of occupants and movable elements cause an extreme variability of geometry and acoustic properties. This requires the ACC filters to be very robust in order to achieve good quality sound zoning for all considered configurations.

4.1 Experimental Setup

A linear loudspeaker array was mounted on the car ceiling in front of the two front seats, as shown in Fig.4. The goal of this experiment was to achieve sound separation between the driver and the passenger. The array was designed to hold *twenty-four 37* mm loudspeakers with a center-to-center distance of *40* mm. Their operative frequency ranges from 300Hz to 12kHz.

To measure the transfer function between the loudspeaker array and the target zones two sets of *twenty 25* mm-spaced microphones, in a linear configuration, were placed in the bright (driver position) and in the dark zone (front passenger position), respectively, at the listener's ears height. In order to analyse the sound zoning performance in real conditions a second set of transfer functions was measured at the ears of the two front passengers, using binaural microphones arranged on the ears of human subjects, as shown in Fig. 5. The control filters based on the first set of transfer functions (i.e. the one measured with the microphone array) were evaluated, in term of acoustic contrast, using the second set of transfer functions (i.e. the one measured with the binaural microphones), as described in section 2.1.1.

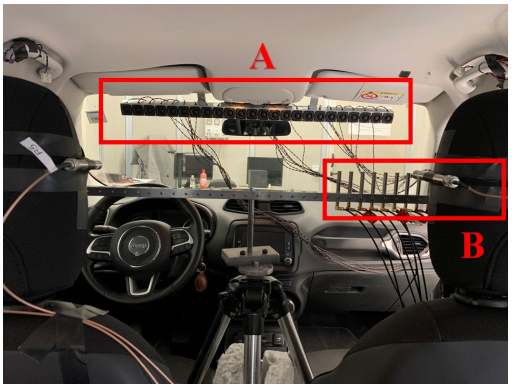

Fig. 4: In-car setup showing (A) the loudspeaker array and (B) the microphone array placed in the dark zone

Fig. 5: Two front passengers wearing the binaural microphones (note that the doors were kept closed during the measurements in order to consider a operative condition)

4.2 Signal Processing

The transfer function estimation was performed by means of the exponential sine sweep method [11]. The $\{\mathbf{G}_B, \mathbf{G}_D\}$ matrices include the transfer functions between loudspeakers and the two set of *twenty* microphones, whereas the transfer function matrices $\{\mathbf{G'}_B, \mathbf{G'}_D\}$ were measured through the two couple of binaural microphones. The second set was generated by repeating the measurements five times and moving the seats by 3 cm back and forth with 1.5 cm step in order to evaluate the robustness of the solution. All measurements were carried out using a sampling frequency of 51.2kHz.

Standard ACC control filters $\mathbf{u}$ were computed according to equation (5) and considering $\{\mathbf{G}_B, \mathbf{G}_D\}$ while the acoustic contrast performances were evaluated with equation (8) and considering the binaural measurements $\{\mathbf{G'}_B, \mathbf{G'}_D\}$.

After that, the identification of the optimal window length for the impulse response trimming was performed by considering a set of forty $\{\tilde{\mathbf{G}}_B, \tilde{\mathbf{G}}_D\}$ matrices, generated by trimming the corresponding impulse responses with forty frequency-independent windows with length varying between 30 and 1200 samples. The optimal window length N^{oct} was then defined for each frequency range as the length that maximizes $\mathbf{AC}^{oct}$ at the binaural microphones.

5 Results

The frequency analysis on the $\mathbf{AC}^{oct}$ variation with respect to the window length has allowed for the evaluation of the impulse responses trimming effect on the sound zoning performance. The example in Figure 6 shows that the acoustic contrast between the two zones in the mid-high frequency range (between 1kHz and 4kHz) is improved by neglecting the impulse response components after 300 samples. In the high frequency range (above 4kHz) the performance is increased by considering only the first 50 samples of the transfer function. On the other hand, an extreme trim can be detrimental in the mid-low frequency range, where the optimal acoustic contrast is reached considering at least 1000 samples (Fig. 6).

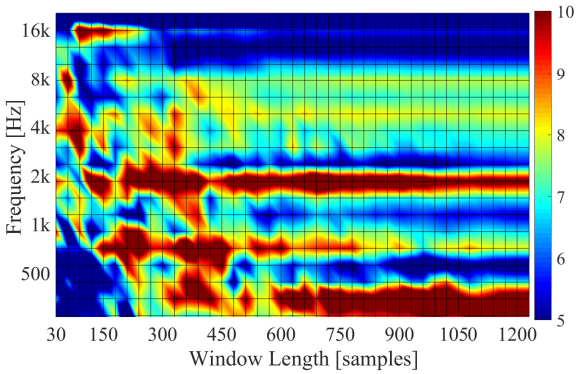

Fig. 6: $\mathbf{AC}^{oct}$ [dB] as a function of the trimming window length for one of the five $\{\mathbf{G'}_B, \mathbf{G'}_D\}$ transfer function matrices

Table 1: Optimal N^{oct} values for various third-octave frequency bands

N^{oct} [samples]	Third-Octave Bands
1000	250Hz−1kHz
300	1.2kHz−3.5kHz
50	4kHz−16kHz

The analysis of the acoustic contrast variation depending on the application of different trimming windows length to five measurements sets estimated at the binaural microphones $\{\mathbf{G'}_B, \mathbf{G'}_D\}$, has led to the optimal frequency-dependent trim. Since no relationship between N^{oct} and $\mathbf{AC}^{oct}$ is evident from the results, three optimal values of N^{oct} have been defined for three different frequency ranges as reported in Table 1. Once the optimal frequency-dependent filtering has been performed, as described in Section 3, the ACC control filters performance, in terms of $\mathbf{AC}^{oct}$, have been com-

pared to the one based on the non-trimmed impulse responses. In Figure 7 the experimental results are shown by averaging the acoustic contrast on the five sets of binaural measurements.

Although only a modest acoustic contrast improvement can be observed, the quality of the control filters $\mathbf{u}$ benefits from the removal of the reverberant component of the IR. In fact, the average of the energy second moment I of the filter impulse responses decreases as shown in Table 2. This is an indicator of the improvement of the filter compactness in the time domain, due to the suppression of the pre and post-ringing components. On the other hand, as shown in Figure 9, the differences in the effort $AE(\mathbf{u})$ between the filters based on the entire transfer function and the frequency-dependent trimmed ones are negligible at frequencies below 7 kHz . At higher frequencies the effort of the non-trimmed filters is 5dB higher.

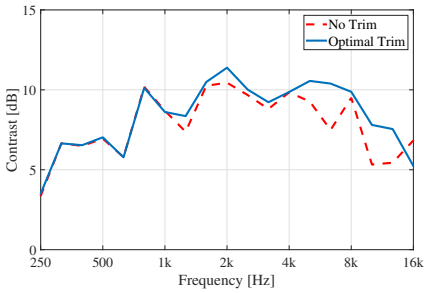

Fig. 7: Average values of $\mathbf{AC}^{oct}$ performed considering the frequency-dependent trimmed impulse responses (blue line) and the entire transfer function (dashed red line)

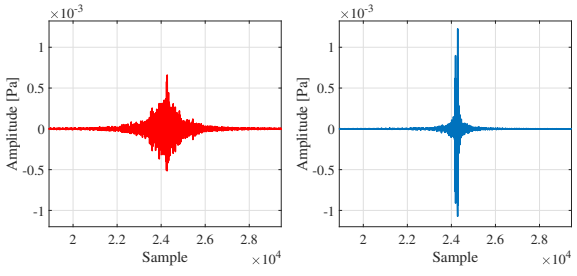

(a) **(b)**

Fig. 8: Inverse filter for loudspeaker n.5 compute with the entire impulse responses (a) and with trimmed impulse responses (b)

Table 2: Averaged energy second moment I of the control filter impulse responses

Control Filters	I
Filters based on $\{\mathbf{G}_B, \mathbf{G}_D\}$	$4.49 \cdot 10^5$
Filters based on $\{\tilde{\mathbf{G}}_B, \tilde{\mathbf{G}}_D\}$	$1.40 \cdot 10^5$

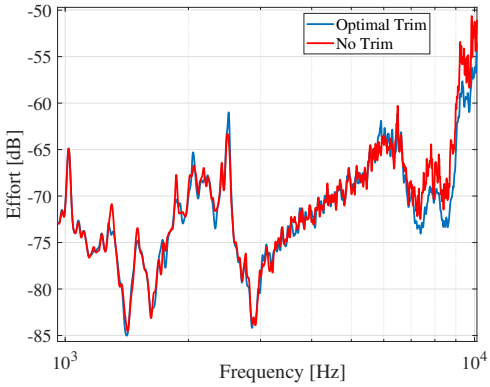

Fig. 9: Effort AE computed considering the frequency-dependent trimmed impulse responses (blue line) and considering the entire transfer function (red line)

6 Conclusions

An innovative technique to optimize the ACC-based control filters has been presented. The proposed method increases the ACC performance and leads to a better sound zoning system based on real measurements. This is obtained by removing the late reflections from the measured impulse responses used for the filter computation. The late reflections may vary significantly with small environmental changes and may lead to unstable acoustic contrast performance when the system operating configuration is different from the one used to compute the control filters. For the experiments presented in this paper the acoustic contrast improvement is more significant in the high frequency range (above 3kHz), where in-car transfer functions have high variability. On the contrary, computing the filters with shortened impulse responses leads to worse acoustic contrast performance at lower frequencies.

This particular impulse response trimming approach is effective also on the control filters quality. It has

indeed been demonstrated that the late reflections suppression from the measured transfer functions lead to more compact and smoother control filters in the time domain. These are expected to results in a higher perceived quality of the reproduced audio, even though this would need to be verified with subjective tests.

The proposed trimming approach could be helpful for sound zoning applications in very reverberant scenarios or in environments with significant geometrical and physical variabilities (e.g. the car cockpit), as it may lead to improved sound separation performance at high frequencies and audio quality.

Future work will investigate the frequency-dependent trim effect on the perceived audio quality in the bright zone and the annoyance in the dark zone by means of listening tests. A further analysis on the effect of the proposed optimization method for specific environment and geometric changes, such as the car windows opening and the variation of the passenger number, is needed in order to statistically define the relation between the optimal trimming length and the frequency. Moreover, it will be investigated the frequency-dependent trim effect on impulse responses to compute PM sound field synthesis. A possible approach would be to relax the constraint of imposing an ideal target sound field, as this would be impossible to be reproduced in real scenarios and may lead to audio artefacts and poor robustness of control filters.

References

[1] Kirkeby, O., Nelson, P. A., Hamada, H., and Orduna-Bustamante, F., "Fast deconvolution of multichannel systems using regularization," *IEEE Transactions on Speech and Audio Processing*, 6(2), pp. 189–194, 1998.

[2] Choi, J.-W. and Kim, Y.-H., "Generation of an acoustically bright zone with an illuminated region using multiple sources," *The Journal of the Acoustical Society of America*, 111, pp. 1695–700, 2002, doi:10.1121/1.1456926.

[3] Simón Gálvez, M. F. and Elliott, S. J., "The Design of a Personal Audio Superdirective Array in a Room," in *Audio Engineering Society Conference: 52nd International Conference: Sound Field Control - Engineering and Perception*, 2013.

[4] Olik, M., Francombe, J., Coleman, P., Jackson, P. J. B., Olsen, M., Møller, M., Mason, R., and Bech, S., "A Comparative Performance Study of Sound Zoning Methods in a Reflective Environment," in *Audio Engineering Society Conference: 52nd International Conference: Sound Field Control - Engineering and Perception*, 2013.

[5] Cheer, J., Elliott, S. J., and Gálvez, M. F. S., "Design and Implementation of a Car Cabin Personal Audio System," *J. Audio Eng. Soc*, 61(6), pp. 412–424, 2013.

[6] Yanagidate, N., Cheer, J., Elliott, S., and Toi, T., "Car Cabin Personal Audio: Acoustic Contrast with Limited Sound Differences," in *Audio Engineering Society Conference: 55th International Conference: Spatial Audio*, 2014.

[7] Goose, S., Riddle, L., Fuller, C., Gupta, T., and Marcus, A., "PAZ: In-Vehicle Personalized Audio Zones," *IEEE MultiMedia*, 23(4), pp. 32–41, 2016.

[8] Elliott, S. J., Cheer, J., Choi, J., and Kim, Y., "Robustness and Regularization of Personal Audio Systems," *IEEE Transactions on Audio, Speech, and Language Processing*, 20(7), pp. 2123–2133, 2012.

[9] Zhu, Q., Coleman, P., Wu, M., and Yang, J., "Robust Acoustic Contrast Control with Reduced In-situ Measurement by Acoustic Modeling," *J. Audio Eng. Soc*, 65(6), pp. 460–473, 2017.

[10] Cho, W.-H. and Chang, J.-H., "Consideration on the Design of Multi-Zone Control System in a Vehicle Cabin," in *Audio Engineering Society Convention 146*, 2019.

[11] Farina, A., "Simultaneous Measurement of Impulse Response and Distortion with a Swept-Sine Technique," in *Audio Engineering Society Convention 108*, 2000.